Thermochimica Acta, 41 (1980) 93—105
Elsevier Scientific Publishing Company, Amsterdam — Printed in Belgium

CHARACTERIZATION OF HYDROCARBON WAXES AND POLYETHYLENES BY DSC

RON MILLER

Perkin-Elmer Corporation, 10805 Sunset Office Drive, St. Louis, MO 63127 (U.S.A.)

GLEN DAWSON

H.B. Fuller Company, 2267 Como Avenue, St. Paul, MN 55108 (U.S.A.)

(Received 17 March 1980)

ABSTRACT

Thermal analysis, originally the technique of DTA, and more recently that of DSC, has been proposed as a means of characterizing waxes. Alternative methods of analysis (refractive index, infrared spectroscopy, etc.) give only a limited amount of information when applied to hydrocarbon waxes. DSC, on the other hand, not only offers a means of distinguishing between microcrystalline, paraffinic, Fischer—Tropsch synthetic, and polyethylene waxes, but offers a scheme by which various hydrocarbon waxes may be fingerprinted. Good agreement between DSC data and the TAPPI system, which utilizes melting point and refractometry, is demonstrated.

INTRODUCTION

Waxes have long been used as components of polishes, paper and container coatings, candles and crayons, and hot melt adhesives. Hot melts is the term given to a class of solvent-free adhesives which require heating to produce fluidity and tack, and cooling to "set". Hot melt cements may vary from tacky, pressure-sensitive formulations to hard, tough solids which develop tack only when melted. They are used to bond a wide variety of substrates, one of which is often paper.

Waxes used in hot melts are most often hydrocarbons, rather than natural products; the most likely wax constituents are paraffins, refined from paraffinic petroleum distillates, and microcrystalline waxes, recovered from distillate residues. Fischer—Tropsch synthetic waxes, resulting from the condensation of hydrogen and carbon monoxide over high pressure catalysts, enjoy increasing popularity, and even petrolatums derived from high viscosity petroleum distillate fractions have been used for certain applications.

Since subtle differences in the wax will result in significant variations in the adhesive and melt rheological properties of the finished hot melt, an accurate and reproducible method of characterizing these waxes is of key importance in the analysis of hot melt cements. Infrared spectroscopic techniques serve to identify the presence of a hydrocarbon wax in an adhesive

0040-6031/80/0000—0000/$02.25

formulation, but cannot discriminate between the various types of hydrocarbon wax. Separation of the *n*-alkanes of a paraffin wax by gas chromatography results in a highly accurate classification technique for paraffins, but is not applicable to the higher boiling microcrystalline or Fischer—Tropsch waxes. Complex classification schemes based on refractive index, congealing point, and kinetmatic viscosity measurements [1,2] tend to be unwieldly, lacking in discriminatory power, and unuseable for very high melting waxes.

An ideal method of wax characterization must not only be rapid and highly discriminating, but should be a micro technique, since pure waxes can, in general, only be completely separated from the polymers used in hot melt adhesives by the use of preparative size exclusion chromatography. These constraints suggest the use of differential scanning calorimetry as the analytical technique of choice. This concept is not new. Lange and Jochinke [3] and Currell and Robinson [4] suggested the possibility as early as 1965. Their work and that of Mazee [5] and Craig et al. [6] was performed on more primitive DTA equipment; the use of DSC was not reported in the literature until 1973, when Giavarini and Pochetti reported the characterization of petroleum products using a Perkin-Elmer DSC-1 [7]. A comprehensive scheme for the characterization of hydrocarbon waxes by thermal analysis has not been previously reported in the literature.

It is the intent of this work to demonstrate the utility of a DSC classification technique for hydrocarbon waxes, and to compare correlations of melt refractive index and DSC-derived melting points with those obtained by Ferris using an ASTM congealing point measurement [1].

EXPERIMENTAL

The thermograms in this study were obtained on a Perkin-Elmer DSC-2 equipped with an Intracooler-II subambient accessory and a Tektronix TEK-31 programmable calculator. Due to the reproducibility and uniformity of the cooling rate obtainable with this system, reproducible thermograms were obtained in both the programmed heating and programmed cooling modes. The wax samples, typically 10—15 mg, were weighed on a microbalance and encapsulated in aluminum pans using the Perkin-Elmer sample encapsulating press. A crimped, empty pan was used as a reference.

Heating rates of 10°C min^{-1} and range settings of 10—20 mcal sec^{-1} $(10\ mV)^{-1}$ were used to obtain melting thermograms, while cooling rates of 5°C min^{-1} and range settings of 5—10 were used for the crystallization thermograms; these conditions appeared to offer a good compromise between speed, resolution, sensitivity, and minimization of the effects of supercooling for the sample size used in the analysis. The usual practice was to run an initial scan at a heating rate of 20°C min^{-1} at a range setting of 20 to premelt the sample and establish the proper range settings and integration limits for the analytical runs. Changes in quenching rate, starting temperature, and holding time did not noticeably affect the melting thermograms.

Refractive indices of wax melts were measured on a Valentine refractometer controlled at 100°C by a circulating water bath filled with a one-to-one

mixture by volume of water and ethylene glycol.

Waxes examined in this work were commercially available materials from Moore and Munger, Bareco, Sonneborne, Mobil, Shell, and other suppliers. Work was performed at the analytical laboratories of the H.B. Fuller Company, St. Paul, Minnesota, U.S.A.

The thermograms obtained in the cooling mode have been replotted with inverted temperature axes so as to align with the temperature axes of the heating curves in the thermograms presented here.

RESULTS AND DISCUSSION

Thermograms of paraffin waxes of the type shown in Fig. 1 have been described in the literature [4,6,7]. Two features are evident: the large peak corresponding to the crystalline melt, and a small peak corresponding to a solid—solid transition. Normal hydrocarbons with chain lengths between 21 and 39 carbon atoms are known to exhibit a transition from an orthorhombic to a hexagonal crystal structure upon heating, while hydrocarbons with chain lengths outside this range crystallize directly into the orthorhombic structure and the transition is not seen.

Wax A in Fig. 1 shows the typical degree of resolution between the solid—solid transition and the melt. The degree of resolution was found to be characteristic of the wax itself, since even very low heating rates did not result in a return to baseline between the transitions for wax A. The solid—solid transition may be more or less resolved from the melt, as in waxes B and C, Fig. 1. Two transition points, as in wax D, Fig. 2, have been observed, and even a reproducible recrystallization exotherm below the melt, as in wax E.

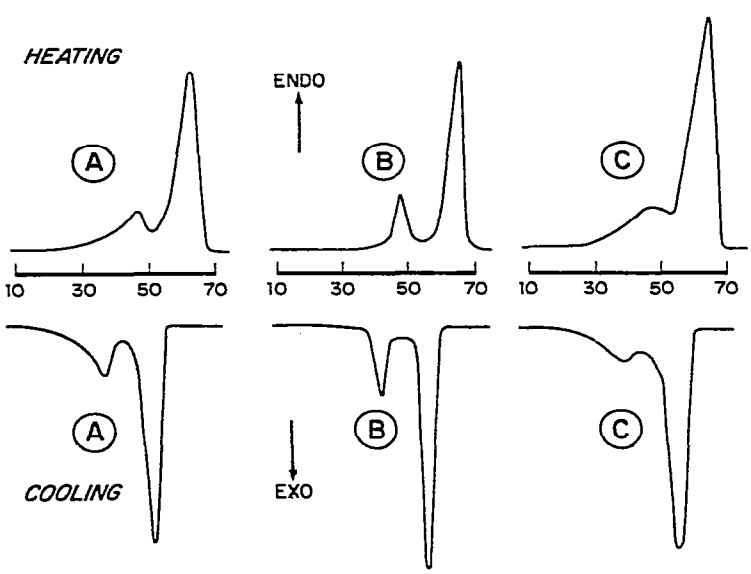

Fig. 1. Thermograms of typical type 1 paraffin waxes.

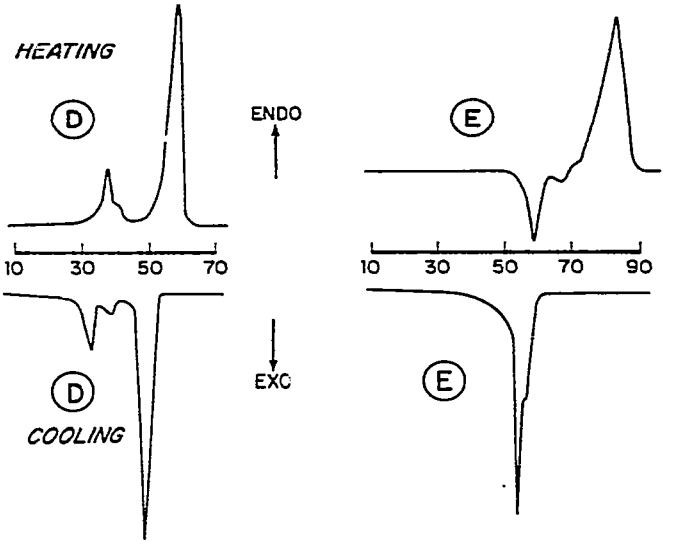

Fig. 2. Thermograms of less typical type 1 paraffin waxes.

These waxes, which are referred to here as type 1 paraffins, typically have total heats of transition between 40 and 50 cal g^{-1}, with most of the values falling between 44 and 48 cal g^{-1}. Peak widths, measured at one half the height of the melt peak, are from 5 to 8° C. With the exception of wax E, the only wax in the entire study exhibiting the recrystallization phenomenon, measured heats of transition agreed to within 3% between heating and cooling measurements on a given wax; this was found true for all types of hydrocarbon waxes studied. For wax E, the area of the endothermic peak obtained on heating is equal to the sum of the areas of the exothermic peaks obtained in both modes, as is expected.

Figure 3 shows a plot of refractive index of the melt plotted against the peak temperature obtained in the heating mode for the paraffin waxes, and a

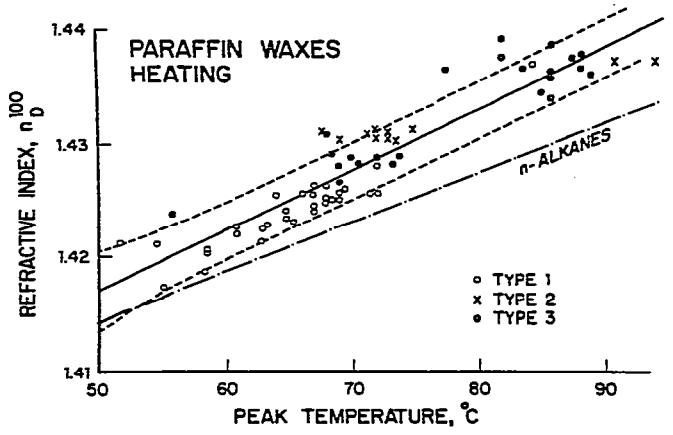

Fig. 3. Plot of melt refractive index vs. peak temperature obtained from heating thermograms of paraffin waxes.

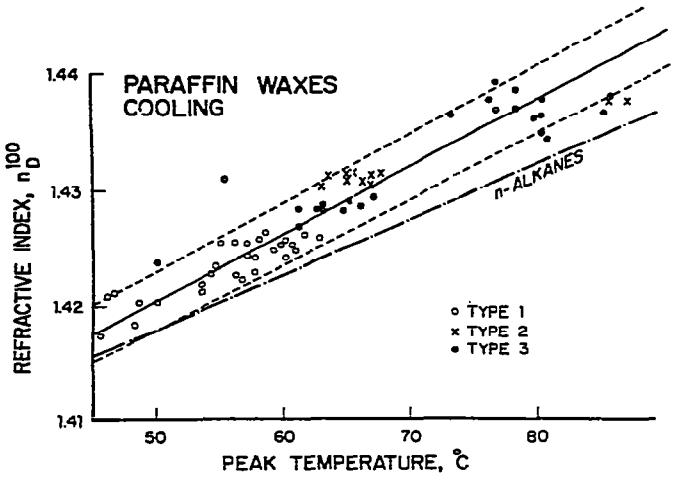

Fig. 4. Plot of melt refractive index vs. peak temperature obtained from cooling thermograms of paraffin waxes.

similar plot for the cooling mode is shown in Fig. 4. The points for the paraffins lie near to but slightly above those for the *n*-alkanes, indicating that the paraffin waxes consist largely of normal alkanes, a fact which appears to be generally conceded in the literature [1].

Figure 5 shows thermograms of a second class of paraffin waxes, referred to here as type 2 paraffins. Heats of transition are the same as for the type 1 paraffins, but peak widths are slightly larger, from 10 to 17°C, due to the incorporation of the solid—solid transition peak into the main peak of the thermogram.

A third type of paraffin wax, the type 3 paraffin, is shown in Fig. 6. Evidence of the solid—solid transition may be absent, as in wax I, apparent only from the programmed cooling curve, as in wax J, or only from the

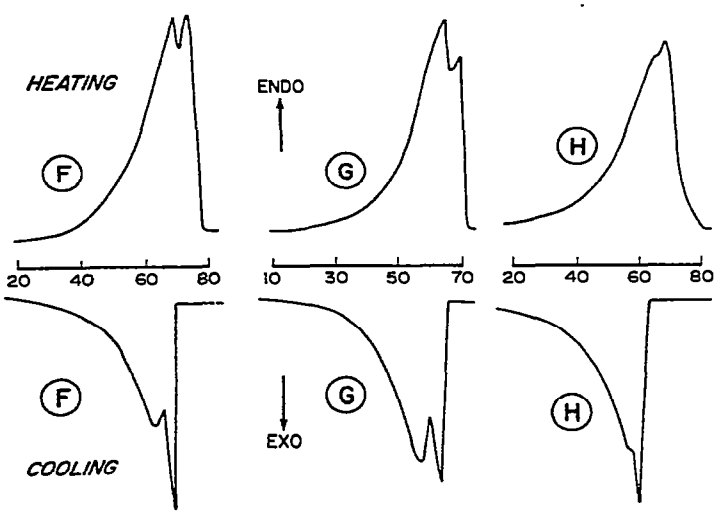

Fig. 5. Thermograms of type 2 paraffin waxes.

programmed heating curve, as in wax K. Loss of the solid—solid transition is expected, as these waxes are higher melting than the type 1 paraffins. Measured heats of fusion are typically the same as for the types 1 and 2 paraffins, but may be as low as 35 cal g^{-1}, possibly due to the inclusion of small amounts of oil in the wax. Peak widths at half-height vary from 7 to 15°C.

Types 2 and 3 paraffins are also plotted in Figs. 3 and 4; their location on the plot indicates that they are indeed paraffins. The solid lines shown in the figures are the regression lines for a least squares linear fit of the data, and have the equations

$$n_D^{100} = 0.000532\ T + 1.3907$$

for the heating mode and

$$n_D^{100} = 0.000586\ T + 1.3913$$

for the cooling mode. The dotted lines describe 95% confidence limits for the regression and will be referred to as the paraffin envelope. As will be seen later, waxes other than paraffins lie outside of the paraffin envelope.

Thermograms of microcrystalline waxes, such as wax L, Fig. 7, have been described by other workers [1,3,4,7]. Microcrystalline waxes may also have bimodal thermograms, as shown for wax M. These shapes are typical, but can be mildly distorted, such as is shown for wax N, Fig. 8, or severely distorted, as in the case of the bimodal wax P.

Microcrystalline waxes are believed to vary but little in molecular weight and to have chains about twice the length of those of paraffins [8]. These carbon chains are doubled back upon themselves to give a hydrodynamic volume similar to that of the paraffins. These waxes may be either soft or hard, and contain high proportions of cyclic, dicyclic, and highly branched alkanes [1].

Measured heats of fusion of the microcrystalline waxes studied varied

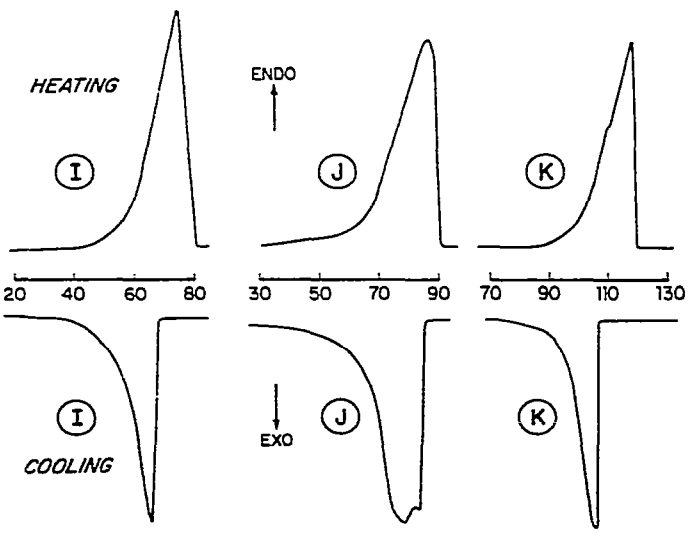

Fig. 6. Thermograms of type 3 paraffin waxes.

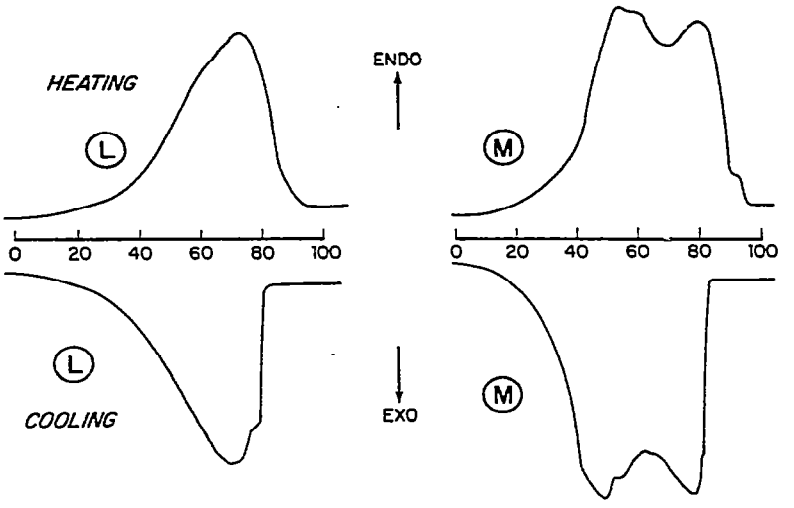

Fig. 7. Thermograms of unimodal (L) and bimodal (M) microcrystalline waxes.

from 30 to 45 cal g^{-1} with the bimodal types all having heats of fusion below 40 cal g^{-1}. Peak widths are typically 20—35° C for unimodal types and 30—50° C for bimodal types. Plots of refractive index vs. peak temperature for heating curves and cooling curves are shown in Figs. 9 and 10, respectively, for 49 unimodal microcrystalline waxes and 22 bimodal waxes. These waxes lie largely above the paraffin envelope, especially in the heating curve data. The shift toward and into the paraffin envelope on the programmed cooling runs can be attributed to a supercooling effect, which is much more prevalent in the less crystalline microwaxes than in the paraffins.

Petrolatums give rise to thermograms somewhat similarly shaped, although the thermograms of wax Z, shown in Fig. 11, are more complex than those of most microcrystalline waxes. Heats of fusion are quite low, 20—30 cal g^{-1}, due to the presence of large amounts of oil, and the peaks are very

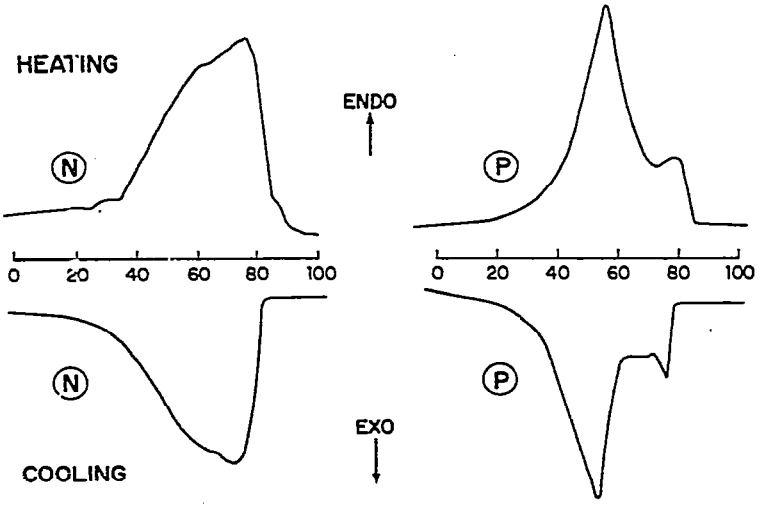

Fig. 8. Thermograms of microcrystalline waxes.

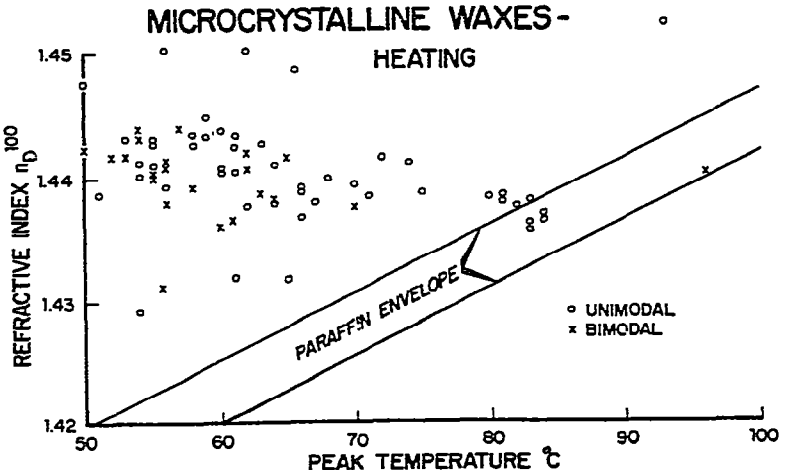

Fig. 9. Plot of melt refractive index vs. peak temperature obtained from heating thermograms of microcrystalline waxes.

broad, typically 50—60°C. Refractive index and thermal data on four petrolatums are given in Table 1.

Figure 12 shows thermograms of typical Fischer—Tropsch synthetic waxes. These waxes are quite brittle, unlike polyethylenes, and have melting endotherms which do not return to the baseline until at or near the high polymer melting point limit; in this manner, they can be distinguished from microcrystalline waxes by DSC alone. Molecular weights can be very high, and waxes similar to R and Q, Fig. 12, can contain a very high percentage of normal alkanes. Other Fischer—Tropsch waxes may have extremely complex melting properties, such as those depicted in Fig. 13. Heats of fusion lie mostly in the range 40- 50 cal g^{-1}, but can fall anywhere between 30 and 55

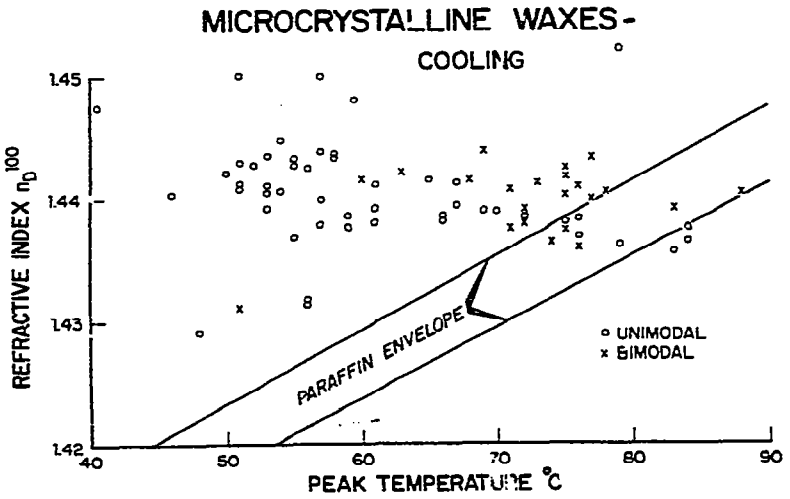

Fig. 10. Plot of melt refractive index vs. peak temperature obtained from cooling thermograms of microcrystalline waxes.

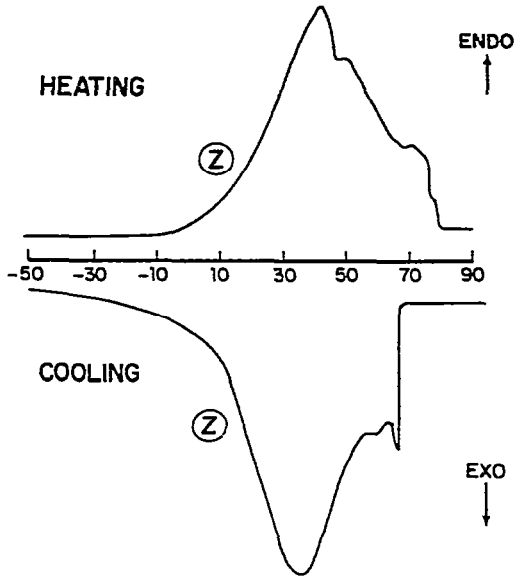

Fig. 11. Thermograms of a petrolatum.

TABLE 1

Refractive index and thermal data for the petrolatums

Sample	n_D^{100}	Peak temperature (°C)	
		Heating	Cooling
W	1.4483	38	32.5
Z	1.4479	40	47
X	1.4450	44	50
Y	1.4500	47.5	42

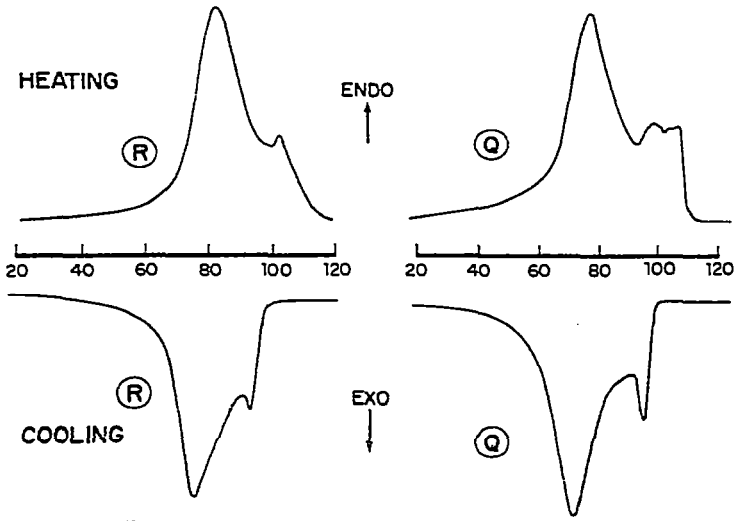

Fig. 12. Thermograms of synthetic waxes.

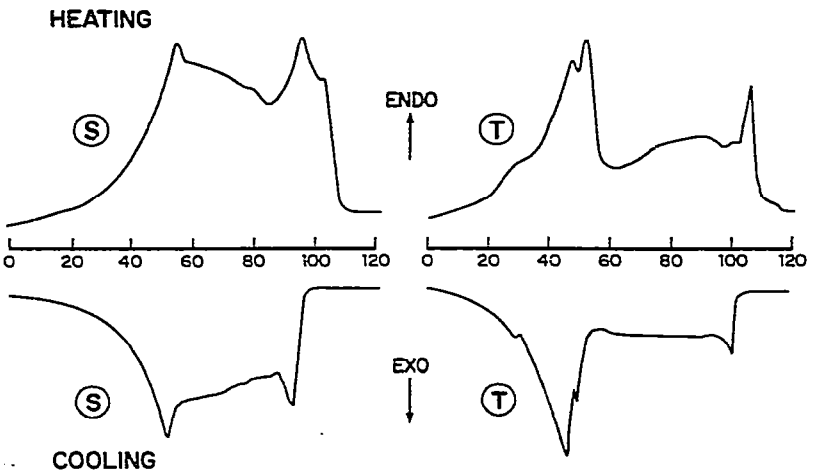

Fig. 13. Thermograms of more complex synthetic waxes.

cal g^{-1}. The heat of fusion appears to vary inversely with the peak width, but the correlation is not good. Peak widths vary from 30 to 80° C.

Figures 14 and 15 show the usual plots of refractive index against peak temperature for 21 Fischer—Tropsch waxes. Although some of the point locations are questionable due to the difficulty of measuring the refractive index of materials still semi-solid at the measurement temperature, leading to high readings, it is apparent that many of these waxes have a high *n*-alkane content; several lie within the paraffin envelope.

Figure 16 shows melting endotherms of two polyethylenes. These materials differ from the synthetic hydrocarbon waxes in both their higher molecular weight and their greater elasticity. The main portion of the melting endotherm is quite narrow, typically only 10—15° C wide, but the

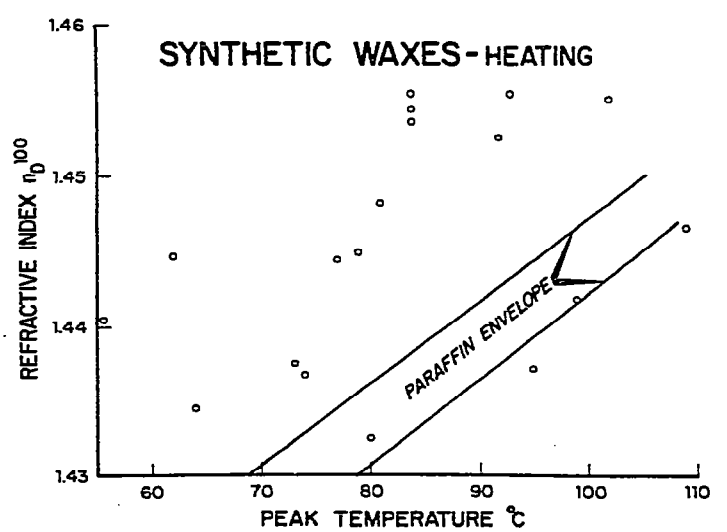

Fig. 14. Plot of melt refractive index vs. peak temperature obtained from heating thermograms of synthetic waxes.

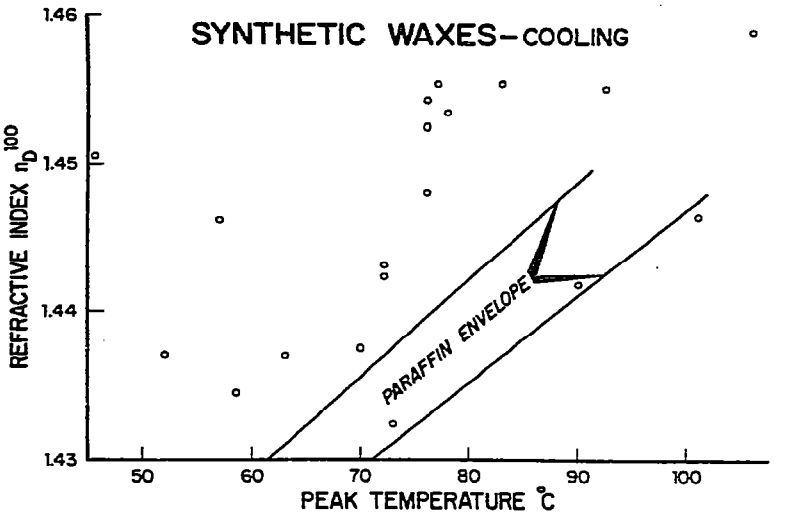

Fig. 15. Plot of melt refractive index vs. peak temperature obtained from cooling thermograms of synthetic waxes.

gradual increase in heat capacity prior to the melt makes integration difficult. Heats of fusion range from 20 to 45 cal g^{-1}. Refractive index data were not obtained, as most of these materials do not even begin to melt at 100° C.

CONCLUSIONS

It has been shown that various types of hydrocarbon waxes yield thermograms of distinct shapes. Figures 17 and 18 show various regimes for heating and cooling data, together with the paraffin envelope and the line cited by Ferris [1] as the dividing line between paraffin waxes and microcrystalline waxes in his classification scheme based on refractive index, congealing point, and kinematic viscosity. It appears that the method of Ferris would

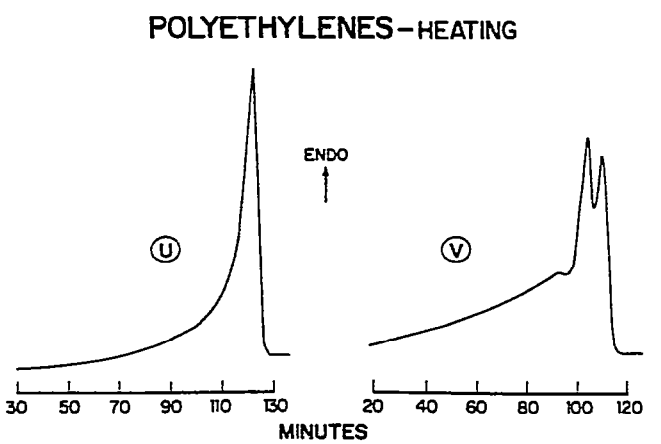

Fig. 16. Heating thermograms of polyethylenes.

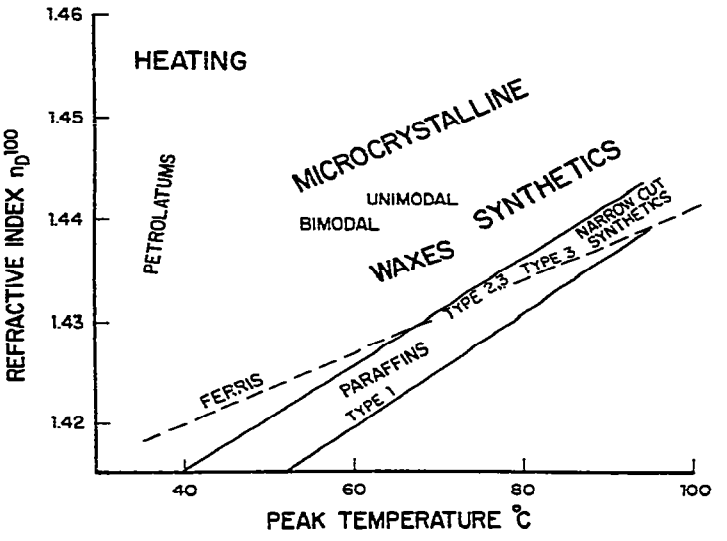

Fig. 17. Regimes of various waxes on a plot of melt refractive index vs. peak temperature obtained in the heating mode.

classify some of the type 2 and type 3 paraffins as microcrystalline waxes, whereas a scheme based on DSC would relegate these materials to the correct groups.

A good procedure would involve establishing and maintaining a library of thermograms of known reference materials, and using it in much the same manner as the spectroscopist would use a library of infrared or NMR spectra. Wax thermograms can be roughly classified into one of the above groups according to shape, peak width, and melting point, and then further identi-

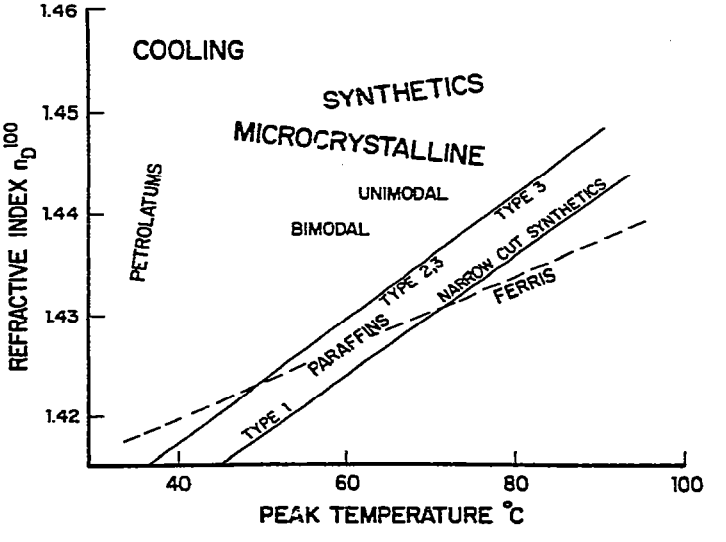

Fig. 18. Regimes of various waxes on a plot of melt refractive index vs. peak temperature obtained in the cooling mode.

fied by matching the subtler features of the curves to the reference thermograms. The procedure has been found to work quite well for waxes isolated from hot melt adhesives.

REFERENCES

1 S.W. Ferris, Special Technical Association Publication No. 2, Technical Association of the Pulp and Paper Industry, 1963, pp. 1—19.
2 J.F. Johnson, Ind. Eng. Chem., 46 (1954) 1046.
3 J. Lange and H. Jochinke, Fette, Seifen, Anstrichm., 67 (1965) 89.
4 B.R. Currell and B. Robinson, Talanta, 14 (1967) 421.
5 W.M. Mazee, Anal. Chim. Acta, 17 (1957) 97.
6 R.G. Craig, J.M. Powers and F.A. Peyton, J. Dent. Res., 46 (1967) 1090.
7 C. Giavarini and F. Pochetti, J. Therm. Anal., 5 (1973) 83.
8 A.H. Warth, The Chemistry and Technology of Waxes, Reinhold, New York, 2nd edn., 1956.